

# Volatile organic compounds enhancing sulfuric acid-based ternary homogeneous nucleation: The important role of synergistic effect

Yu Zhao<sup>a</sup>, Yi-Rong Liu<sup>a</sup>, Shuai Jiang<sup>a</sup>, Teng Huang<sup>b</sup>, Zi-Hang Wang<sup>a</sup>, Cai-Xin Xu<sup>a</sup>, Ya-Juan Feng<sup>a, \*\*</sup>, Wei Huang<sup>a,b,c,\*</sup>

<sup>a</sup> School of Information Science and Technology, University of Science and Technology of China, Hefei, Anhui, 230026, China

<sup>b</sup> Laboratory of Atmospheric Physico-Chemistry, Anhui Institute of Optics & Fine Mechanics, Chinese Academy of Sciences, Hefei, Anhui, 230031, China

<sup>c</sup> CAS Center for Excellent in Urban Atmospheric Environment, Xiamen, Fujian, 361021, China



## HIGHLIGHTS

- Nucleation capability of ternary system is stronger than that of binary system.
- Ternary clusters are more stable than binary clusters due to synergistic effect.
- Synergistic effect reduces evaporation and stabilizes pre-nucleation clusters.

## ARTICLE INFO

**Keywords:**  
Nucleation mechanism  
Synergistic effect  
Atmospheric relevance  
Evaporation rate  
Proton transfer

## ABSTRACT

New particle formation (NPF) is an important source of atmospheric aerosols. Sulfuric acid (SA) and water (W) are recognized as essential participating substances in the nucleation of the atmosphere. In addition, as one of the most common organic acids, oxalic acid (OA) can improve NPF when amine such as methylamine (MA) is present. However, exploring the properties of atmospheric particles made up of different components is challenging and the role of volatile organic compounds in SA-based ternary homogeneous nucleation is still lacking in research. In this work, the structures and energies of  $(SA)_x(OA)_y(MA)_z(W)_m$  ( $0 \leq x, y, z \leq 3, 0 \leq m \leq 1$ ) are investigated. The results indicate that it is accessible for SA to form clusters with OA and MA molecules through hydrogen bonds and proton transfer interactions. The analysis of non-covalent interactions and proton transfer reveals that ternary nucleation systems have stronger hydrogen bonds and more proton transfers than binary systems to stabilize the clusters. In terms of the thermodynamic properties, the Gibbs free energies of the clusters will decrease as the addition of SA, OA or MA molecules indicating that the synergistic effect of these three substances may be of potential in forming the initial cluster and subsequent growth processes. Moreover, the evaporation rates of clusters show that the synergistic effect of ternary clusters leads to a decrease in evaporation rate which may promote atmospheric nucleation.

## 1. Introduction

Atmospheric aerosols affect our life deeply, including reducing visibility, influencing environment and climate, as well especially endangering human health (Charlson et al., 1992; Kulmala, 2003; Kittelson et al., 2004; Saxon and Diaz-Sanchez, 2005). In addition to discharging aerosols directly, new particle formation (NPF) is an important source of atmospheric aerosols and dominates concentrations of cloud condensation nuclei (CCN) (Charlson et al., 2001), so it is meaningful for

researchers to understand the mechanism of NPF. The most important issues about NPF consist of the conditions of occurrence, nucleation mechanism, and growth mechanism (Zhang, 2010; Wang et al., 2010; Zhang et al., 2012; Yue et al., 2010). Although some progress has been made in the chemical mechanism of NPF, there are still many uncertain issues remaining to be discussed, especially in the case of multiple components and organic compounds (Kulmala, 2003; Zhang et al., 2004; Kulmala et al., 2012, 2013).

According to experimental and theoretical researches, sulfuric acid

\* Corresponding author. School of Information Science and Technology, University of Science and Technology of China, Hefei, Anhui, 230026, China.

\*\* Corresponding author.

E-mail addresses: [fengyj6@ustc.edu.cn](mailto:fengyj6@ustc.edu.cn) (Y.-J. Feng), [huangwei6@ustc.edu.cn](mailto:huangwei6@ustc.edu.cn) (W. Huang).

( $\text{H}_2\text{SO}_4$ , SA) and water ( $\text{H}_2\text{O}$ , W) are the key members involved in nucleation (Zhang et al., 2012; Bzdek et al., 2012; Kulmala et al., 2004; Schobesberger et al., 2015; Elm, 2017). However, based on a lot of field observations and experimental results, it has been reported that the binary SA/W nucleation system is insufficient to explain the NPF results (Kuang et al., 2010; Kulmala and Kerminen, 2008; Smith et al., 2008; Paasonen et al., 2010). Recently, experimental studies and field observations have listed that the ternary SA/W/ammonia ( $\text{NH}_3$ ) nucleation (Kulmala et al., 2000; Kerminen et al., 2010), ion-induced nucleation (Kirkby et al., 2011), ion-mediated nucleation (IMN) (Yu, 2006; Yu and Turco, 2000; Yu et al., 2018), organic acids (Zhang et al., 2004), organic amines (Nadykto et al., 2015) and highly oxidized multifunctional organic molecules (HOMs) (Li et al., 2017) can improve the nucleation efficiency. And the thermodynamic nucleation of organic acids and amines have been also considered to help explain the high nucleation rate. The acid-base reaction occurs in the clusters of SA- $\text{NH}_3$ /amines, and it is observed to gradually grow by adding the base after SA (Kirkby et al., 2011; Bzdek et al., 2017; Schobesberger et al., 2013). However, researches on the application of acid-base reactions in the formation and growth of nanoparticles and clusters are not clear enough (Barsanti et al., 2009). In this study, these observations are supplemented by theoretical calculations of the ternary nucleation reaction of SA and base with volatile organic compounds.

It is well known that in recent years, the emission of volatile organic compounds (VOCs) has increased rapidly (He et al., 2019), and VOCs usually play an important role in NPF. Increasing evidences have shown that the condensation of low VOCs is critical for NPF (Metzger et al., 2010; Ling et al., 2019). Although organics in particulate matters have been observed from continent to ocean (Jimenez et al., 2009; Karl et al., 2012), which means that they may be factors of great importance in NPF by stabilizing small clusters for further growth (Arquero et al., 2017), their specific impacts on NPF are still remaining to be discovered. Dicarboxylic acids are common organic acids which mainly come from automobile exhaust, photochemical reactions and some emissions (Prenni et al., 2001). Since dicarboxylic acids are of relatively low vapor pressure and sufficient solubility, they can easily participate in nucleation (da Silva et al., 1999; Makar, 2001). Low molecular weight dicarboxylic acids have been detected as major organic compounds in aerosol and rainwater samples (Saxena and Hildemann, 1996; Kawamura and Ikushima, 1993). Zhang et al. have pointed out that the presence of organic acids can significantly promote the nucleation of SA (Zhang et al., 2004). And previous studies (Nadykto and Yu, 2007; Xu et al., 2010a, 2010b) have shown that some low weight molecular organic acids can combined with SA to participate in nucleation and are believed to be involved in NPF. As one of the most common dicarboxylic acid, oxalic acid ( $\text{C}_2\text{H}_2\text{O}_4$ , OA) was observed to get a gas phase concentration at about the range of  $9.3 \times 10^{10}$  to  $5.4 \times 10^{12} \text{ cm}^{-3}$  (Martinelango et al., 2007; Miao et al., 2015; Liu et al., 1996). In field observations (Liu et al., 1996), the concentration of oxalate originated from OA has a strong correlation with CNN. And OA can form positively charged and stable sulfuric acid-oxalic acid-water complexes to participate in nucleation of atmospheric ions (Xu et al., 2010a). In the meanwhile, earlier researches have revealed that SA or methanesulfonic acid (MSA) can effectively bind with methylamine ( $\text{CH}_3\text{NH}_2$ , MA) to form particles in the atmosphere (Bustos et al., 2014; Lv et al., 2015; Chen et al., 2016; Chen and Finlayson-Pitts, 2017; Yu et al., 2012; Glasoe et al., 2015). MA, as one of the most important organic amines diffusing in the world (Smith et al., 2008, 2010; Almeida, 2013; Kurten et al., 2008; Loukonen et al., 2010; Nadykto et al., 2011; Schade and Crutzen, 1995; Zhao et al., 2011), can enhance the nucleating ability of SA. The global emission concentration of MA is  $83 \pm 26 \text{ Gg N a}^{-1}$ , which is twice the emission concentration of dimethylamine ( $\text{CH}_3\text{NHCH}_3$ , DMA). It has increased significantly under the situations of animal husbandry, biomass burning and oceans (Ge et al., 2011a; Cornell et al., 2003). McGregor et al. (McGregor and Anastasio, 2001) also reported the discovery of methylamine in fog water collected in California. Studies on

the thermodynamic properties of amines have shown that methylamine can react with acids in the atmosphere to form very low vapor pressure compounds, which can participate in nucleation or NPF (Ge et al., 2011b). Moreover, Arquero et al. (2017) and Xu et al. (2017) have studied the role of the clusters of OA, MSA, MA and W in the NPF. Experimental and theoretical calculations have verified that the addition of OA can moderately promote the nucleation of the (MSA)(MA) mixtures. Therefore, the role of OA in the nucleation of (SA)(MA) clusters deserves studying.

Recently, the formation and growth of multicomponent particles in the atmosphere have gradually become hot spots (Xu et al., 2017; Liu et al., 2018; Zhang et al., 2017; Myllys et al., 2019). Although organic matter is widespread in the air and they are predicted to participate in NPF, the role of volatile organic compounds in SA-based ternary homogeneous nucleation is still unclear. This work mainly studies the nucleation mechanism of  $(\text{SA})_x(\text{OA})_y(\text{MA})_z(\text{W})_m$  ( $0 \leq x, y, z \leq 3, 0 \leq m \leq 1$ ) and the important role of synergistic effects in atmospheric nucleation. The equilibrium structures of  $(\text{SA})_x(\text{OA})_y(\text{MA})_z(\text{W})_m$  ( $0 \leq x, y, z \leq 3, 0 \leq m \leq 1$ ) are calculated by the Basing Hopping algorithm (Yoon et al., 2007; Wales and Doye, 1997; Huang et al., 2010a) coupled with density functional theory (DFT) at M06-2X/6-311++G (3df, 3pd) level. Then we discuss the non-covalent interactions and proton transfer of clusters because the properties of clusters such as structures and binding energies have a great correlation with whether protons will transfer from acid to base. Furthermore, the thermodynamic properties of the (SA)(OA)(MA) clusters and the interactions of different components are researched to reveal synergistic effects at the molecule level. Finally, considering quantum chemical calculation and dynamic simulation by Atmospheric Cluster Dynamics Code (ACDC) (McGrath et al., 2012), the evaporation rates of the clusters are investigated to determine whether the clusters are stable in the atmosphere.

## 2. Theoretical methods

In this study, based on the Basing Hopping (BH) algorithm and density functional theory (DFT), the structures and thermodynamics properties of  $(\text{SA})_x(\text{OA})_y(\text{MA})_z(\text{W})_m$  ( $0 \leq x, y, z \leq 3, 0 \leq m \leq 1$ ) clusters are calculated. This method is efficient and accurate when searching for geometry optimization, in the meantime, it has been widely used in previous studies of atomic and molecular systems (Huang et al., 2010b, 2010c; Liu et al., 2014; Xu et al., 2013; Wen et al., 2014; Lin et al., 2014). The BH algorithm generates configurations by random displacement of atoms and then optimizes to local minimum structures. For each cluster, the BH algorithm search consists of 1000-step sampling and is performed 3 times. The initial structural spaces are originally generated with Boltzmann weight at the initial temperature. The initial structures within 6 kcal mol<sup>-1</sup> gap of the lowest energy configuration are selected to be optimized. The global minimum and local minimum structures of each cluster is obtained using M06-2X method (Zhao and Truhlar, 2008; Elm et al., 2013; Zhang et al., 2019) with 6-311++G(3df, 3pd) basic set (Nadykto and Yu, 2007; Xu et al., 2010a). Finally, thermodynamic parameters including the binding energy (E), enthalpy (H) and the Gibbs free energy (G) were evaluated at the M06-2X/6-311++G (3df, 3pd) level. Gaussian 09 program is used for geometry and frequency calculations to make sure that there is no imaginary frequency for each stationary point (Frisch et al., 2013).

In early works, M06-2X has a brilliant performance on the prediction of kinetics, structures and noncovalent interactions (Zhao and Truhlar, 2008) and has excellent consistency in predictions with cluster formation experimental results (Elm et al., 2012). In order to evaluate the performance of the chosen method, the results calculated by M06-2X/6-311++G(3df, 3pd) were compared with experimental results (Hanson and Eisele, 2000, 2002; Hanson and Lovejoy, 2006). The calculation details were briefly discussed in Table S1. The use of M06-2X/6-311++G(3df, 3pd) in thermodynamic prediction are found to be in good agreement with the experimental results. Therefore, based

on the consideration of calculation cost, the M06–2X/6–311++G(3df, 3pd) theoretical level is chosen to guarantee accuracy and efficiency.

### 3. Results and discussion

#### 3.1. Structures analysis

According to the number of molecular species, the structures can be divided into unitary, binary, ternary and hydration clusters. The global minimum structures of the binary clusters  $(OA)_x(MA)_y$ ,  $(SA)_x(OA)_y$  and  $(SA)_x(MA)_y$  ( $1 \leq x, y \leq 3$ ) optimized at the M06–2X/6–311++G(3df, 3pd) level are displayed in Fig. 1. The most stable structures of the ternary clusters and their hydration clusters  $(SA)_x(OA)_y(MA)_z(W)_m$  ( $1 \leq x, y, z \leq 2, 0 \leq m \leq 1$ ) at the M06–2X/6–311++G(3df, 3pd) level are shown in Fig. 2.

For binary clusters, no proton transfer occurs in the  $(OA)_1(MA)_1$  cluster and this cluster is mainly stabilized by a N···H–O hydrogen bond with a bond distance of 1.54 Å and an intermolecular O–H···O bond with length of 1.98 Å inside the OA are formed. Then, OA and MA are added to the dimer, which are  $(OA)_2(MA)_2$  and  $(OA)_3(MA)_3$  in Fig. 1, the proton transfer between the hydroxyl of OA and the nitrogen of MA is occurred by forming an  $[HC_2O_4]^-[CH_3NH_3]^+$  ion pair. Moreover, the global minimum of  $(SA)_1(OA)_1$  cluster forms two H···O hydrogen bonds between SA and OA with length of 1.72 Å and 1.75 Å in the  $(SA)_1(OA)_1$  cluster. It is obvious that proton transfer occurs in  $(SA)_1(MA)_1$  cluster, one N–H···O hydrogen bond with length of 1.40 Å is formed between SA and MA in  $(SA)_1(MA)_1$  cluster. For the hydrates of binary clusters displayed in Fig. S1, the combination of acid and base occur proton transfer to form  $[HC_2O_4]^-[CH_3NH_3]^+$  or  $[HSO_4]^-[CH_3NH_3]^+$  ion pairs after the addition of water molecules. In addition, the structure gradually changes from ring structures to more complex cage structures as the

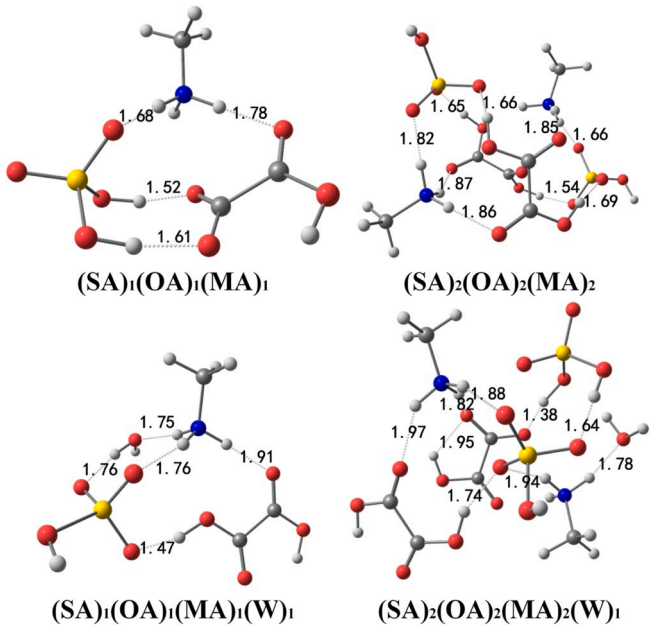


Fig. 2. The optimized geometries of  $(SA)_x(OA)_y(MA)_z(W)_m$  ( $1 \leq x, y, z \leq 2, 0 \leq m \leq 1$ ) at the M06–2X/6–311++G(3df, 3pd) level.

number of molecules increases.

For the  $(SA)_1(OA)_1(MA)_1$  cluster, three monomers form a ring structure where proton transfer occurs between OA and MA. The hydrogen bond length between OA and MA is 1.78 Å, the hydrogen bond length between SA and MA is 1.68 Å and two hydrogen bonds with

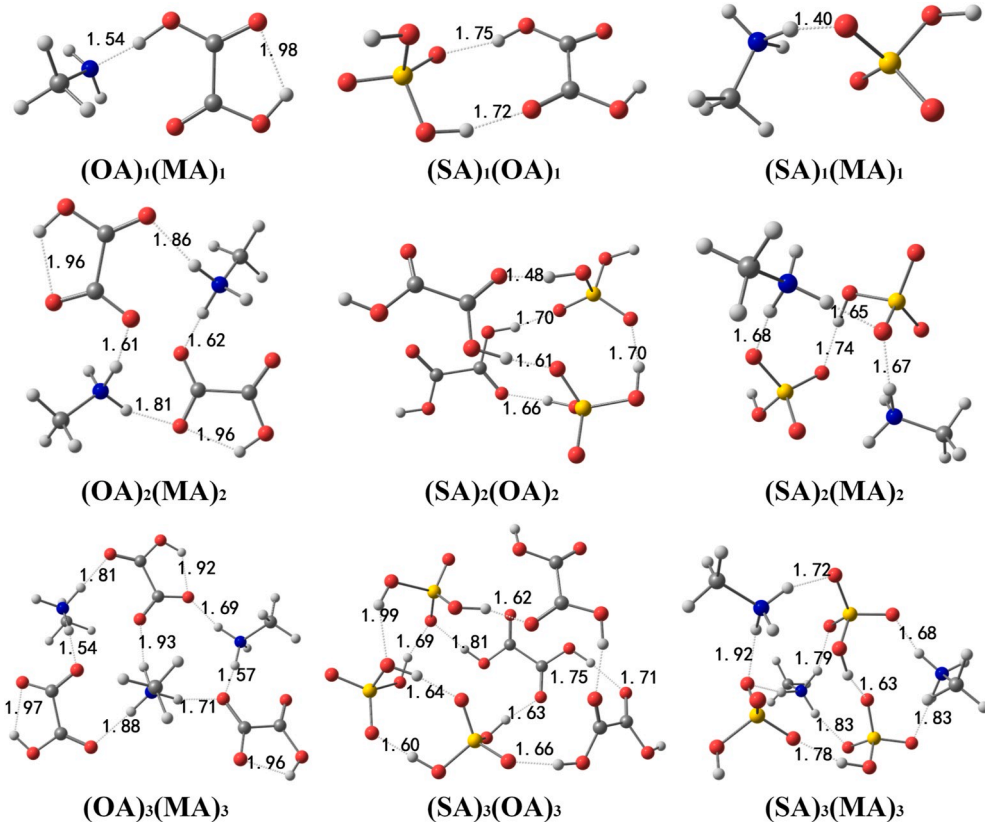


Fig. 1. The optimized geometries of  $(OA)_x(MA)_y$ ,  $(SA)_x(OA)_y$  and  $(SA)_x(MA)_y$  ( $1 \leq x, y \leq 3$ ) at the M06–2X/6–311++G(3df, 3pd) level (red for oxygen, white for hydrogen, gray for carbon, blue for nitrogen and yellow for sulfur). (For interpretation of the references to color in this figure legend, the reader is referred to the Web version of this article.)

length of 1.52 Å and 1.61 Å are formed between SA and OA. The structures of  $(SA)_2(OA)_2(MA)_2$  and  $(SA)_2(OA)_2(MA)_2(W)_1$  are both complicated cage structures. When water molecules are added, the number of hydrogen bonds increases. In addition, other ternary structures can be found in the Supporting Information.

In conclusion, SA can form clusters with OA and MA through hydrogen bonds and proton transfers. Proton transfer occurs when water molecules are added or another substances are involved in nucleation. As the number of substances increases, the structure becomes more and more complex and the number of hydrogen bonds increases as well.

### 3.2. Analysis of noncovalent interactions and proton transfer

The noncovalent interaction (NCI) index was proposed by Yang and coworkers (Johnson et al., 2010) to describe the relationship between the reduced density gradient and electron density. The  $s$  refers to the reduced density gradient (RDG) indicating deviation from the uniform distribution of electrons (Hohenberg and Kohn, 1964; Cohen et al., 2008). According to former researches, it is useful to determine and visualize the non-covalent interactions, so it can be used to compare the intermolecular non-covalent interactions between the  $(SA)(OA)(MA)(W)$ -based clusters.

$$s = \frac{1}{2(3\pi^2)^{1/3}} \frac{|\nabla\rho|}{\rho^{4/3}} \quad (1)$$

Where  $\nabla$  is the gradient operator and  $|\nabla\rho|$  is the electron density gradient mode. The analysis of NCIs of  $(SA)_x(OA)_y(MA)_z(W)_m$  ( $0 \leq x, y, z \leq 3, 0 \leq m \leq 1$ ) is carried out using the above formula. By using the Multiwfns (Lu and Chen, 2012) and VMD (Humphrey et al., 1996) programs, the plots of the RDG ( $s$ ) vs. the electron density ( $\rho$ ) multiplied by the sign of the second Hessian eigenvalue ( $\lambda_2$ ) and bonding isosurfaces for the  $(OA)_1(MA)_1$ ,  $(OA)_1(MA)_1(W)_1$ ,  $(SA)_1(OA)_1(MA)_1$  and  $(SA)_1(OA)_1(MA)_1(W)_1$  are shown in Fig. 3. The plots of other clusters can be seen in Fig. S4 and Fig. S5.

The values of  $\text{sign}(\lambda_2)\rho$  are the indicators for judging the strength of interaction. When the value of  $\text{sign}(\lambda_2)\rho$  is negative, the interaction forms a hydrogen bond, and when the value of  $\text{sign}(\lambda_2)\rho$  gradually increases to nearly zero, the interaction gradually weakens, like van der Waals force. And the positive value of  $\text{sign}(\lambda_2)\rho$  represents the interaction is a hindrance. The colors of the plots of RDG( $s$ ) and bonding isosurfaces represent the strength of the interaction. Blue represents hydrogen bonds, green represents van der Waals forces, and red represents steric hindrance. As can be seen from the figure, the ternary system and the hydration system get more and stronger hydrogen bonds than the binary system. The reduced gradient isosurface and scatter plots are consistent with the analysis of the structural section.

Moreover, depending on the strength of the acid and base, proton transfer occurs from the acid molecules to the base molecule in the acid-base clusters (Xu et al., 2017). The proton-transfer parameters, (Liu et al., 2018) (Kurnig and Scheiner, 1987; Hunt et al., 2003)  $\rho_{PT}$ , the degree of proton transfer across the hydrogen bond is employed to evaluate the degree of ionization based on the distance between atoms.

$$\rho_{PT} = (r_{OH} - r_{OH}^0) - (r_{H-N} - r_{H-N}^0) \quad (2)$$

Where  $r_{OH}$  and  $r_{OH}^0$  are the distances of hydrogen bond in the OA or SA in the clusters and the O-H distance in the monomers, respectively.  $r_{H-N}$  and  $r_{H-N}^0$  are the distances of hydrogen bond in the  $(SA)_x(OA)_y(MA)_z(W)_m$  ( $0 \leq x, y, z \leq 3, 0 \leq m \leq 1$ ) clusters and the H-N distance in the  $\text{CH}_3\text{NH}_3^+$  ion after proton transfer, respectively. For clusters in which the proton transfer does not occur, the first term is approximately zero and in this case  $\rho_{PT}$  will appear to be negative. For clusters that fully transferred proton transfer interaction take place, the second term is zero and  $\rho_{PT}$  is a positive number.

Table 1 lists a part of the proton transfer parameters of

$(SA)_x(OA)_y(MA)_z(W)_m$  ( $0 \leq x, y, z \leq 3, 0 \leq m \leq 1$ ), others can refer to Table S2. For the  $(OA)_1(MA)_1$  dimer, its proton transfer parameter  $\rho_{PT}$  is negative and combined with the previous hydrogen bond analysis, it can be confirmed that no proton transfer occurs and only one hydrogen bond exists between OA and MA. However, when the acid is SA and the base is MA, proton transfer occurs and forms an  $[\text{HSO}_4]^-[\text{CH}_3\text{NH}_3]^+$  ion pair, in which SA is the proton donor and MA is the acceptor. For ternary clusters and hydration clusters, the proton transfer parameters are positive and proton transfer occurs in all cases. Generally, the number of proton transfers does not exceed the number of MA molecules in the cluster.

Previous studies (Arquero et al., 2017) have reported that the role of water molecules in enhancing NPF is attributed to the following two mechanisms: increasing the amount of hydrogen bonding or enhancing proton transfer. In this work, the number of hydrogen bond increases as water molecules are added and water molecules play an important role in the occurrence of proton transfer. Furthermore, through analysis of non-covalent effects and proton transfer parameters, two apparent conclusions can be obtained: first, as the number of atoms increasing or the addition of water molecules, the number of hydrogen bonds, the complexity of geometry and the number of proton transfers increase. Second, protons can be supplied by SA and transfer to MA, but in some clusters, protons can transfer from OA to MA as well.

### 3.3. Thermodynamics of the cluster formation

The nucleation mechanism is very important in the atmospheric aerosol research, and the nucleation rate is closely related to the free energies (Zhang et al., 2012). Thermodynamic properties have important implications for the analysis of intermolecular interactions and their spontaneous formation (Peng et al., 2015). Table 2 and Table 3 illustrate that the thermodynamic parameters of the clusters including the binding energy changes ( $\Delta E^{0K}$ ), the intermolecular enthalpies ( $\Delta H^{298.15K}$ ) and the Gibbs free energy changes ( $\Delta G^{298.15K}$ ) at the M06-2X/6-311++G(3df, 3pd) level. Table 2 presents the thermodynamic parameters of  $(OA)_x(MA)_y$ ,  $(SA)_x(OA)_y$  and  $(SA)_x(MA)_y$  ( $1 \leq x, y \leq 3$ ) from the constituent monomers. It can be seen that the  $\Delta G$  value of  $(SA)_1(MA)_1$  is  $-8.12 \text{ kcal mol}^{-1}$ , which has the lowest  $\Delta G$  value compared to another two dimers. Based on this, we can figure out that among the three dimers  $(OA)_1(MA)_1$ ,  $(SA)_1(OA)_1$  and  $(SA)_1(MA)_1$ , SA and MA are more easily combined to form cluster, which is consistent with the above conclusions that proton transfer only exists in the  $(SA)_1(MA)_1$  dimer. Moreover, it can be seen that the  $\Delta G$  value grows more negative when  $(OA)_1(MA)_1$ ,  $(SA)_1(OA)_1$  and  $(SA)_1(MA)_1$  continue to grow up which means the  $\Delta G$  value of  $(OA)_1(MA)_1 > (OA)_2(MA)_2 > (OA)_3(MA)_3$  and it is exactly the same for  $(SA)(MA)$  and  $(SA)(OA)$  systems, so  $(OA)_3(MA)_3$ ,  $(SA)_3(MA)_3$  and  $(SA)_3(OA)_3$  are easily formed in thermodynamics, respectively. From the thermodynamic properties of hydrated clusters in Table S3, it can be concluded that  $(SA)(OA)$  and  $(SA)(MA)$  clusters can combine with water molecules to form clusters. The special cases are the clusters based on  $(OA)(MA)$ , which are difficult to form hydrated clusters by adding water molecules.

The thermodynamic parameters of  $(SA)_x(OA)_y(MA)_z(W)_m$  ( $1 \leq x, y, z \leq 2, 0 \leq m \leq 1$ ) are shown in Table 3. From the perspective of  $\Delta G$  values, the  $\Delta G$  value of the ternary structure is more negative than any dimer structures. This implies that the addition of a substance will have a synergistic effect on the binary structure, especially for the  $(OA)_1(SA)_1$  dimer, the addition of MA can greatly promote its nucleation. In the subsequent growth, these three basic molecules can still be added. For hydrated clusters, the  $\Delta\Delta G$  value ( $\Delta G$  value of hydrate minus  $\Delta G$  value of non-hydrate) increases from  $-3.65 \text{ kcal mol}^{-1}$  to  $-0.67 \text{ kcal mol}^{-1}$ , indicating that it is increasingly difficult to add water molecules as the clusters become larger.

Fig. 4 shows the variation of Gibbs free energy with the number of SA, OA, and MA, revealing the synergistic effect of SA on the NPF of  $(OA)(MA)$  system. The  $\Delta G$  values of the clusters sharing same amount of

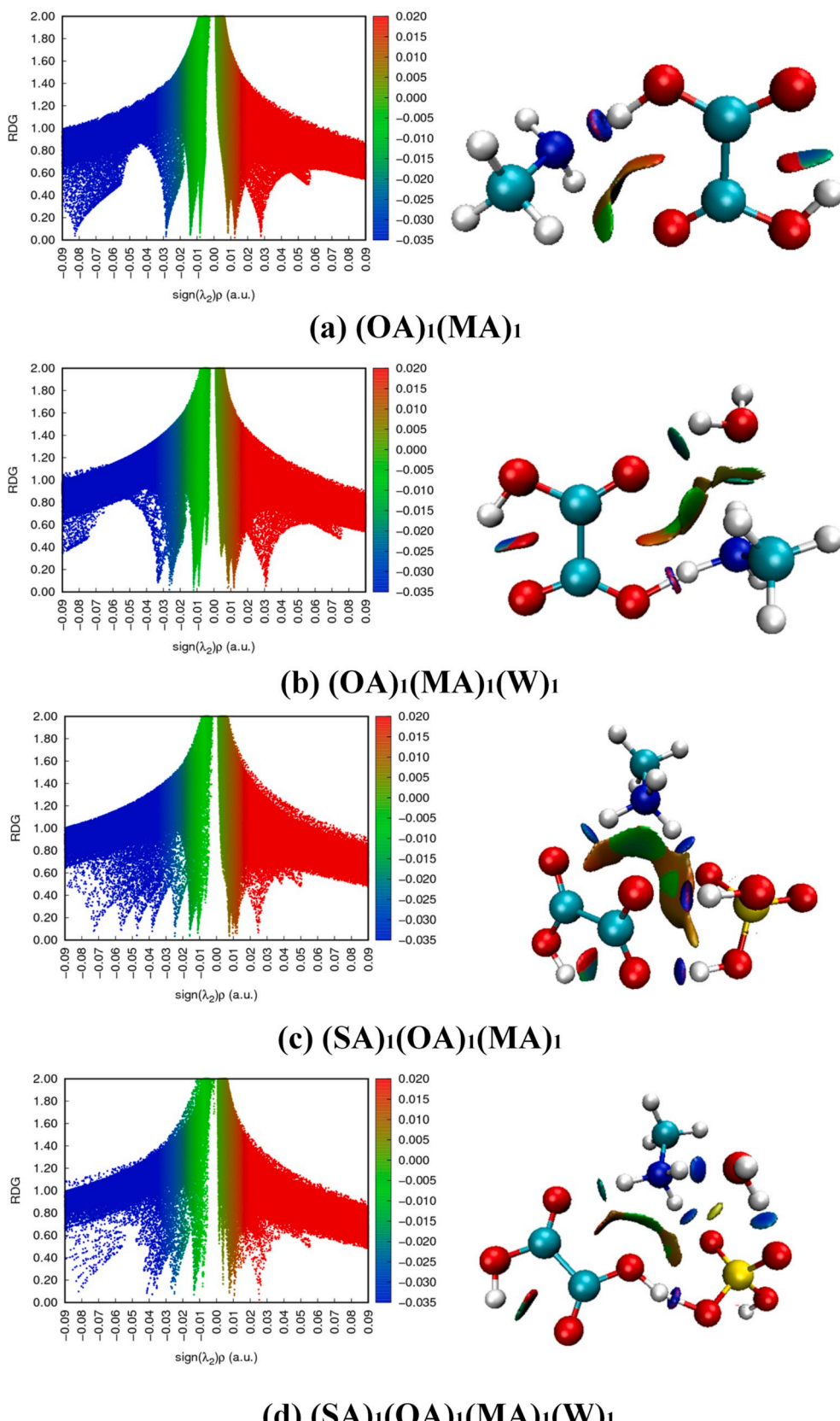


**Fig. 3.** Non-covalent interactions (NCI) analysis among the global minima for (a)  $(\text{OA})_1(\text{MA})_1$ , (b)  $(\text{OA})_1(\text{MA})_1(\text{W})_1$ , (c)  $(\text{SA})_1(\text{OA})_1(\text{MA})_1$ , (d)  $(\text{SA})_1(\text{OA})_1(\text{MA})_1(\text{W})_1$ .

**Table 1**

Proton transfer parameter ( $\rho_{PT}$ , Å) for (SA)(OA)(MA)(W)-based clusters.  $r_{OH}$  and  $r_{H...N}$  (Å) are the bond distances between the O and H atoms and that between the H and N atoms, respectively.

Clusters	$r_{OH}$ (Å)	$r_{H...N}$ (Å)	$\rho_{PT}$ (Å)	Proton donor
(OA) <sub>1</sub> (MA) <sub>1</sub>	1.050	1.540	-0.429	-
(OA) <sub>1</sub> (MA) <sub>1</sub> (W) <sub>1</sub>	1.367	1.148	0.280	OA
(SA) <sub>1</sub> (MA) <sub>1</sub>	1.485	1.400	0.151	SA
(SA) <sub>1</sub> (MA) <sub>1</sub> (W) <sub>1</sub>	1.522	1.080	0.508	SA
(SA) <sub>1</sub> (OA) <sub>1</sub> (MA) <sub>1</sub>	1.781	1.040	0.802	OA
(SA) <sub>1</sub> (OA) <sub>1</sub> (MA) <sub>1</sub> (W) <sub>1</sub>	1.765	1.038	0.793	SA
(SA) <sub>2</sub> (OA) <sub>2</sub> (MA) <sub>2</sub>	1.823	1.448	0.441	SA
	1.656	1.048	0.674	SA
(SA) <sub>2</sub> (OA) <sub>2</sub> (MA) <sub>2</sub> (W) <sub>1</sub>	2.031	1.024	1.068	OA
	1.878	1.030	0.914	SA

**Table 2**

The thermodynamic parameters (kcal mol<sup>-1</sup>) of (OA)<sub>x</sub>(MA)<sub>y</sub>, (SA)<sub>x</sub>(OA)<sub>y</sub> and (SA)<sub>x</sub>(MA)<sub>y</sub> (1 ≤ x, y ≤ 3) from the constituent monomers. The energies are calculated at the M06-2X/6-311++G(3df, 3pd) level.

Reactions	$\Delta E(0\text{ K})$	$\Delta H(298.15\text{ K})$	$\Delta G(298.15\text{ K})$
SA+OA→(SA) <sub>1</sub> (OA) <sub>1</sub>	-13.61	-13.36	-3.71
OA+MA→(OA) <sub>1</sub> (MA) <sub>1</sub>	-14.51	-14.62	-4.66
SA+MA→(SA) <sub>1</sub> (MA) <sub>1</sub>	-18.53	-18.92	-8.12
2SA+2OA→(SA) <sub>2</sub> (OA) <sub>2</sub>	-40.74	-40.06	-6.12
2OA+2MA→(OA) <sub>2</sub> (MA) <sub>2</sub>	-47.92	-47.93	-16.31
2SA+2MA→(SA) <sub>2</sub> (MA) <sub>2</sub>	-69.15	-69.58	-36.17
3SA+3OA→(SA) <sub>3</sub> (OA) <sub>3</sub>	-75.15	-74.62	-13.98
3OA+3MA→(OA) <sub>3</sub> (MA) <sub>3</sub>	-80.73	-80.17	-28.76
3SA+3MA→(SA) <sub>3</sub> (MA) <sub>3</sub>	-121.38	-121.89	-64.94

**Table 3**

The thermodynamic parameters (kcal mol<sup>-1</sup>) of the (SA)<sub>x</sub>(OA)<sub>y</sub>(MA)<sub>z</sub>(W)<sub>m</sub> (1 ≤ x, y, z ≤ 2, 0 ≤ m ≤ 1) from the constituent monomers. The energies are calculated at the M06-2X/6-311++G(3df, 3pd) level.

Reactions	$\Delta E(0\text{ K})$	$\Delta H(298.15\text{ K})$	$\Delta G(298.15\text{ K})$
SA+OA+MA→(SA) <sub>1</sub> (OA) <sub>1</sub> (MA) <sub>1</sub>	-38.37	-38.82	-15.95
2SA+2OA+2MA→(SA) <sub>2</sub> (OA) <sub>2</sub> (MA) <sub>2</sub>	-102.21	-101.72	-45.15
SA+OA+MA+W→(SA) <sub>1</sub> (OA) <sub>1</sub> (MA) <sub>1</sub> (W) <sub>1</sub>	-49.62	-50.23	-19.60
2SA+2OA+2MA+W→(SA) <sub>2</sub> (OA) <sub>2</sub> (MA) <sub>2</sub> (W) <sub>1</sub>	-113.02	-113.45	-45.82

OA and MA molecules and with zero (red rectangle), one (black circle), two (blue triangle) and three (orange star) SA molecules are ranged from top to bottom on the figure. This indicates that the  $\Delta G$  value of clusters decreases as the SA molecules are added. Regardless of the amount of OA and MA, the nucleation reaction after the addition of SA molecules can spontaneously proceed.

The meaning of the abscissa  $x_{my_n}$  in Fig. 4 is the amount of OA and MA, where x refers to OA and m is the number of OA molecules (m = 0–3), y refers to MA and n is the number of MA molecules (n = 0–3). Analyze this picture from two angles: the first one is based on the number of OA molecules. We take three as a group for comparison, so there are three groups in total, which are (x1y1, x2y1, x3y1), (x1y2, x2y2, x3y2) and (x1y3, x2y3, x3y3). It can be seen that the  $\Delta G$  value decreases as the number of OA molecules increases generally. The second angle is analyzed by the change in the number of MA, it can also be divided into three groups of (x1y1, x1y2 and x1y3), (x2y1, x2y2 and x2y3) and (x3y1, x3y2 and x3y3). Therefore, it can be concluded that the increase in the number of OA and MA molecules may also cause the decrease in the  $\Delta G$  value of clusters.

Fig. 5 shows the specific values of Gibbs free energy for (SA)<sub>x</sub>(OA)<sub>y</sub>(MA)<sub>z</sub> (0 ≤ x, y, z ≤ 3) on the different SA numbers of OA-MA grid. It can be seen that as the substance increases, the  $\Delta G$  value decreases

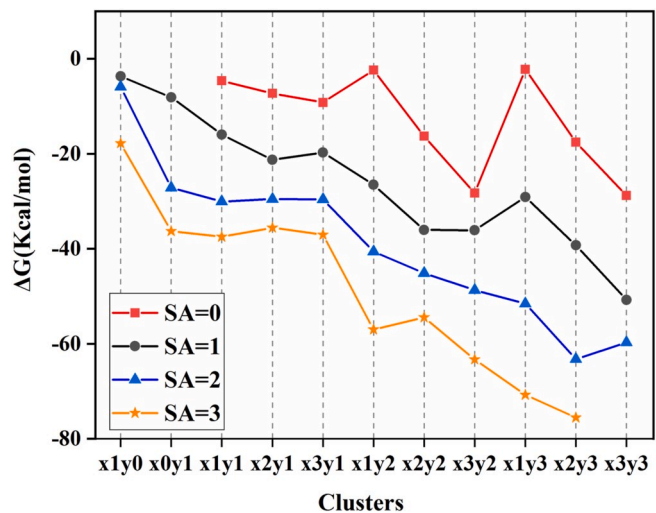


**Fig. 4.** Formation Gibbs free energies ( $\Delta G$ , kcal mol<sup>-1</sup>) of  $x_{my_n}$  clusters ( $x = \text{OA}$ ,  $y = \text{MA}$ ,  $m = 0–3$ ,  $n = 0–3$ ) with zero (red rectangle), one (gray circle), two (blue triangle) and three (orange star) sulfuric acid (SA) molecules at 298.15 K at the M06-2X/6-311++G(3df, 3pd) level. (For interpretation of the references to color in this figure legend, the reader is referred to the Web version of this article.)

constantly and rapidly along the diagonal direction. The synergistic effect of these three substances may be important in forming the initial cluster and subsequent growth processes. At the same time, it can be inferred that the nucleation path may grow along the diagonal direction.

Moreover, previous studies (Loukonen et al., 2010; Kuerten et al., 2014) have shown that DMA can strongly stabilize SA and is conducive to atmospheric nucleation. Table 4 lists the Gibbs free energies of (SA)(OA)(MA) clusters and (SA)(DMA) clusters, which are compared to ensure that the total number of molecules and the number of SA molecules in the clusters are equal. When only one SA molecule exists, the  $\Delta G$  values of the (SA)(OA)(MA) clusters are smaller than (SA)(DMA) clusters, which indicates that the (SA)(OA)(MA) clusters are more stable than (SA)(DMA) clusters in thermodynamics. As the number of SA increases, (SA)(DMA) clusters are more stable than (SA)(OA)(MA) clusters.

In summary, the  $\Delta G$  values of the ternary clusters are smaller than those of the binary clusters, which indicates that the synergistic effects in thermodynamics makes the ternary cluster easier to form. Moreover, the  $\Delta G$  values of the clusters continue to decrease with the addition of SA molecules, and the increment of OA and MA molecules, showing the possibility of clusters continuing to grow along the diagonal. The comparison of Gibbs free energies of (SA)(OA)(MA) clusters and (SA)(DMA) clusters shows that when the number of SA is small, (SA)(OA)(MA) clusters are more stable thermodynamically than (SA)(DMA) clusters.

#### 3.4. Atmospheric relevance

McGrath et al. (2012) proposed the Atmospheric Cluster Dynamics Code (ACDC) to simulate the cluster formation process by considering the thermodynamic properties and dynamic processes of clustering. The simulation results obtained by this method are consistent with the experimental results (Kuerten et al., 2016; Olenius et al., 2013) and can be used for researching nucleation and the corresponding mechanism. In order to evaluate whether the clusters can grow into a larger stable cluster under real steam concentration in the atmosphere, it is not enough to consider only the formation free energy ( $\Delta G$ ) of the cluster formation into consideration. Under certain circumstances, the collision and evaporation rates can be used to infer the stability of the cluster, mainly depending on the collision rate constant and the concentration of acid and base molecules (Elm et al., 2017; Xie et al., 2017; Ma et al.,

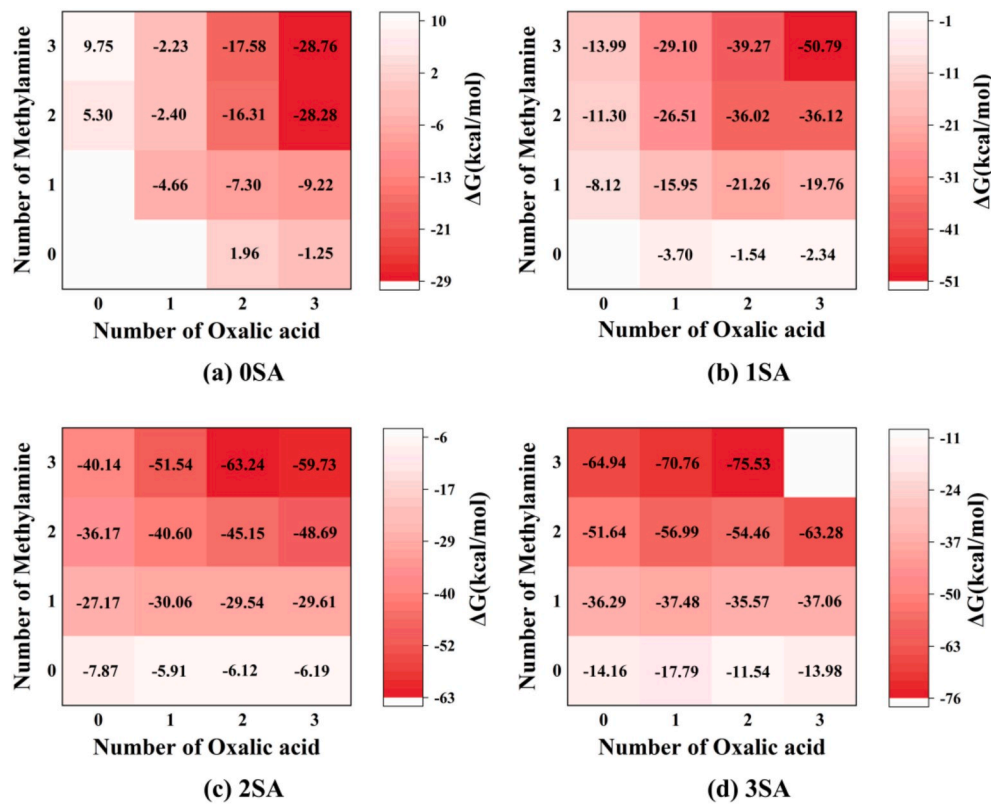


**Fig. 5.** The Gibbs free energies ( $\Delta G$ ,  $\text{kcal mol}^{-1}$ ) for  $(\text{SA})_x(\text{OA})_y(\text{MA})_z$  ( $1 \leq x, y, z \leq 3$ ) on different SA numbers ((a). 0SA, (b). 1SA, (c). 2SA, (d). 3SA) of OA-MA grid at 298.15 K at the M06-2X/6-311++G(3df, 3pd) level.

**Table 4**

The comparison of Gibbs free energies ( $\Delta G$ ,  $\text{kcal mol}^{-1}$ ) of  $(\text{SA})_x(\text{DMA})_y$  ( $1 \leq x, y \leq 3$ ) and  $(\text{SA})_x(\text{OA})_y(\text{MA})_z$  ( $1 \leq x, y, z \leq 3$ ). The energies are calculated at the M06-2X/6-311++G(3df, 3pd) level.

Cluster	$\Delta G$ ( $\text{kcal mol}^{-1}$ )	Cluster	$\Delta G$ ( $\text{kcal mol}^{-1}$ )
$(\text{SA})_1(\text{DMA})_2$	-14.13	$(\text{SA})_1(\text{OA})_1(\text{MA})_1$	-15.95
$(\text{SA})_1(\text{DMA})_3$	-17.36	$(\text{SA})_1(\text{OA})_1(\text{MA})_2$	-26.51
$(\text{SA})_1(\text{DMA})_4$	-15.69	$(\text{SA})_1(\text{OA})_2(\text{MA})_1$	-21.26
		$(\text{SA})_1(\text{OA})_1(\text{MA})_3$	-29.10
		$(\text{SA})_1(\text{OA})_2(\text{MA})_2$	-36.02
		$(\text{SA})_1(\text{OA})_3(\text{MA})_1$	-19.76
$(\text{SA})_2(\text{DMA})_2$	-41.38	$(\text{SA})_2(\text{OA})_1(\text{MA})_1$	-30.06
$(\text{SA})_2(\text{DMA})_3$	-47.23	$(\text{SA})_2(\text{OA})_1(\text{MA})_2$	-40.60
$(\text{SA})_3(\text{DMA})_2$	-57.01	$(\text{SA})_2(\text{OA})_2(\text{MA})_1$	-29.54
		$(\text{SA})_3(\text{OA})_1(\text{MA})_1$	-37.48

2019).

The collision coefficient for clusters i and j is given as (McGrath et al., 2012)

$$\gamma_{ij} = \left(\frac{3}{4\pi}\right)^{1/6} \left(\frac{6k_b T}{m_i} + \frac{6k_b T}{m_j}\right)^{1/2} (V_i^{1/3} + V_j^{1/3})^2 \quad (3)$$

The evaporation coefficient can be calculated from the collision coefficient and the Gibbs free energies (McGrath et al., 2012):

$$\gamma_{(i+j)\rightarrow i} = \beta_{ij} \frac{p_{ref}}{k_b T} \exp\left\{\frac{\Delta G_{i+j} - \Delta G_i - \Delta G_j}{k_b T}\right\} \quad (4)$$

where  $k_b$  is the Boltzmann constant,  $T$  is the temperature in Kelvin,  $m$  is the mass of cluster,  $V$  is the volume of cluster,  $p_{ref}$  is the reference pressure and  $\Delta G$  is the Gibbs free energy of cluster formed by the constituent monomers, respectively.

The evaporation rates of  $(\text{SA})_x(\text{OA})_y(\text{MA})_z$  ( $0 \leq x, y, z \leq 3$ ) on different SA numbers of OA-MA grid at 298.15 K are shown in Fig. 6.

When there is no SA molecule, evaporation rates for clusters  $(\text{OA})_x(\text{MA})_y$  ( $1 \leq x, y \leq 3$ ) are greater than the order of  $10^2 \text{ s}^{-1}$ , which are higher than those for other clusters with SA molecules. The results indicate that SA molecules can promote the stability of  $(\text{OA})(\text{MA})$  clusters in the atmosphere. The evaporation rate of  $(\text{SA})_2(\text{MA})_2$  is  $1.68 \times 10^4 \text{ s}^{-1}$  and after replacing one of the SA molecules with OA molecule,  $(\text{SA})_1(\text{OA})_1(\text{MA})_2$  has a lower evaporation rate of  $1220 \text{ s}^{-1}$ , which means the cluster might appear to be more stable. It can be seen that there is a synergistic effect between SA and OA to promote nucleation. Fig. 7 shows a comparison of the evaporation rates of binary clusters  $(\text{SA})_x(\text{OA})_y$  ( $1 \leq x, y \leq 3$ ) and ternary clusters  $(\text{SA})_x(\text{OA})_y(\text{MA})_z$  ( $1 \leq x, y, z \leq 3$ ) as the molecule number of cluster increases. It can be derived from the figure that in the case where the number of molecules of the cluster is the same, the evaporation rate of the ternary cluster is smaller than that of the binary cluster. In particular, when the number of molecules is 4, the evaporation rate of  $(\text{SA})_2(\text{OA})_2$  is  $5.14 \times 10^{11} \text{ s}^{-1}$ , and the lowest evaporation rate  $(\text{SA})_1(\text{OA})_1(\text{MA})_2$  is  $1220 \text{ s}^{-1}$ , which differs by 8 orders of magnitude. Thus, the participation of MA molecules instead of SA or OA molecule can also reduce the evaporation rate, which indicates that there is a synergistic effect among the three substances to stabilize the clusters.

In conclusion, on the one hand, the addition of SA molecules stabilizes the clusters and reduces the evaporation rate of the clusters. On the other hand, the synergistic effect inside the ternary clusters can significantly reduce the evaporation rate of the binary clusters, making the cluster more stable in the atmosphere. In addition, the synergistic effect of SA and organic components can reduce the  $\Delta G$  value of nucleation to make the cluster easy to form spontaneously. Therefore, ternary clusters can exist in a more stable form in the atmosphere.

#### 4. Conclusions

In this study, the nucleation mechanisms and synergistic effect of

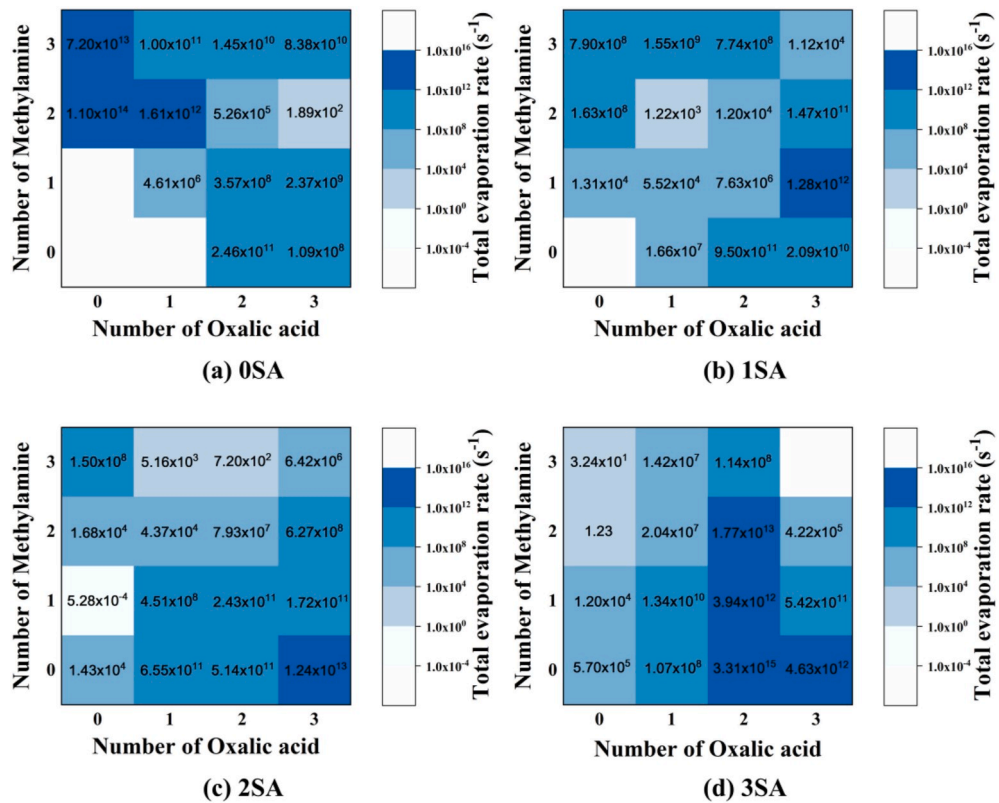


**Fig. 6.** The total evaporation rates for  $(\text{SA})_x(\text{OA})_y(\text{MA})_z$  ( $1 \leq x, y, z \leq 3$ ) on different SA numbers ((a). 0SA, (b). 1SA, (c). 2SA, (d). 3SA) of OA-MA grid at 298.15 K at the M06-2X/6-311++G(3df, 3pd) level.

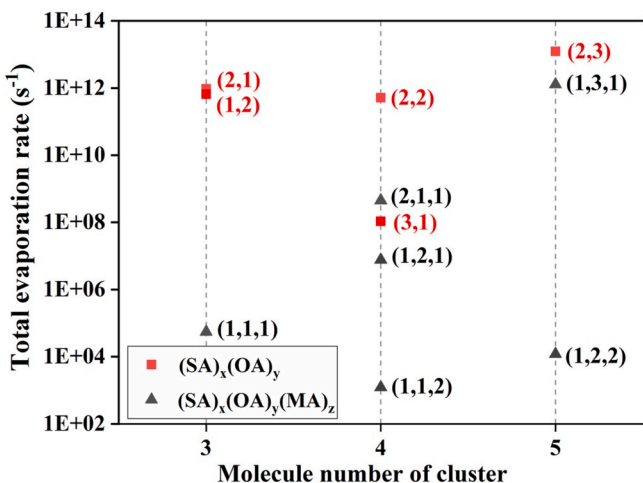


**Fig. 7.** Comparison of the evaporation rate of binary clusters  $(\text{SA})_x(\text{OA})_y$  ( $1 \leq x, y \leq 3$ ) (red rectangle) and ternary clusters  $(\text{SA})_x(\text{OA})_y(\text{MA})_z$  ( $1 \leq x, y, z \leq 3$ ) (gray triangle) as the molecule number of cluster increases at 298.15 K at the M06-2X/6-311++G(3df, 3pd) level. (For interpretation of the references to color in this figure legend, the reader is referred to the Web version of this article.)

$(\text{SA})_x(\text{OA})_y(\text{MA})_z(\text{W})_m$  ( $0 \leq x, y, z \leq 3, 0 \leq m \leq 1$ ) clusters have been researched as the configurations and thermodynamic properties have been calculated. The structures of clusters have showed that SA combines with OA and MA to form clusters by hydrogen bonding and proton transfer. Meanwhile, the analysis of non-covalent interactions and proton transfer has suggested that the ternary structures generate more hydrogen bonds and proton transfers. The thermodynamic properties of clusters have found that the Gibbs free energies of ternary nucleation are

smaller than those of binary nucleation, indicating that the addition of substances has a synergistic effect on the binary structures. And the  $\Delta G$  values of the clusters have been decreasing which shows the potential of clusters continuing to grow. Moreover, by using quantum chemical calculations and dynamic simulation of Atmospheric Cluster Dynamics Code, the total evaporation rate of clusters on OA-MA grids with different SA numbers has been obtained. The addition of SA molecules stabilizes the clusters and ternary clusters have lower evaporation rates than binary clusters, which reveal the synergistic effect between SA and organic components. Understanding the interactions of acids, bases and water molecules in the atmosphere are of essential significance to predict NPF scales accurately. Our research has showed that SA can form clusters with OA and MA through hydrogen bonding and proton transfer and the synergistic effects of SA and organic components can promote nucleation, which have theoretical implications for the nucleation mechanism of SA, OA and MA in the atmosphere.

#### Declaration of competing interest

The authors declare that they have no known competing financial interests or personal relationships that could have appeared to influence the work reported in this paper.

#### CRediT authorship contribution statement

**Yu Zhao:** Conceptualization, Methodology, Data curation, Writing - original draft, Writing - review & editing. **Yi-Rong Liu:** Software, Investigation, Visualization. **Shuai Jiang:** Formal analysis, Data curation. **Teng Huang:** Resources. **Zi-Hang Wang:** Writing - review & editing. **Cai-Xin Xu:** Visualization. **Ya-Juan Feng:** Methodology, Validation, Formal analysis, Writing - review & editing. **Wei Huang:** Methodology, Software, Supervision, Project administration, Funding acquisition.

## Acknowledgments

This work was supported by the National Natural Science Foundation of China (Grant No. 41877305, 21573241, 41605099, 41705097, 41705111, 41775112 and 41527808), the National Science Fund for Distinguished Young Scholars (Grant No. 41725019), the Key Research Program of Frontier Science, CAS (Grant No. QYZDB-SSW-DQC031), the National Key Research and Development program (Grant No. 2016YFC0202203), the National Research Program for Key Issues in Air Pollution Control (DQGG0103) and the Fundamental Research Funds for the Central Universities of China (Grant No. WK2100000008).

## Appendix A. Supplementary data

Supplementary data to this article can be found online at <https://doi.org/10.1016/j.atmosenv.2020.117609>.

## References

- Almeida, J., et al., 2013. Molecular understanding of sulphuric acid-amine particle nucleation in the atmosphere. *Nature* 502, 359–363.
- Arquero, K.D., Gerber, R.B., Finlayson-Pitts, B.J., 2017. The role of oxalic acid in new particle formation from methanesulfonic acid, methylamine, and water. *Environ. Sci. Technol.* 51, 2124–2130.
- Barsanti, K.C., McMurry, P.H., Smith, J.N., 2009. The potential contribution of organic salts to new particle growth. *Atmos. Chem. Phys.* 9, 2949–2957.
- Bustos, D.J., Temelso, B., Shields, G.C., 2014. Hydration of the sulfuric acid-methylamine complex and implications for aerosol formation. *J. Phys. Chem. A* 118, 7430–7441.
- Bzdek, B.R., Pennington, M.R., Johnston, M.V., 2012. Single particle chemical analysis of ambient ultrafine aerosol: a review. *J. Aerosol Sci.* 52, 109–120.
- Bzdek, B.R., DePalma, J.W., Johnston, M.V., 2017. Mechanisms of atmospherically relevant cluster growth. *Accounts Chem. Res.* 50, 1965–1975.
- Charlson, R.J., Schwartz, S.E., Hales, J.M., Cess, R.D., Coakley, J.A., Hansen, J.E., Hofmann, D.J., 1992. Climate forcing by anthropogenic aerosols. *Science* 255, 423–430.
- Charlson, R.J., Seinfeld, J.H., Nenes, A., Kulmala, M., Laaksonen, A., Facchini, M.C., 2001. Atmospheric science - reshaping the theory of cloud formation. *Science* 292, 2025–2026.
- Chen, H., Finlayson-Pitts, B.J., 2017. New particle formation from methanesulfonic acid and amines/ammonia as a function of temperature. *Environ. Sci. Technol.* 51, 243–252.
- Chen, H., Varner, M.E., Gerber, R.B., Finlayson-Pitts, B.J., 2016. Reactions of methanesulfonic acid with amines and ammonia as a source of new particles in air. *J. Phys. Chem. B* 120, 1526–1536.
- Cohen, A.J., Mori-Sanchez, P., Yang, W., 2008. Insights into current limitations of density functional theory. *Science* 321, 792–794.
- Cornell, S.E., Jickells, T.D., Cape, J.N., Rowland, A.P., Duce, R.A., 2003. Organic nitrogen deposition on land and coastal environments: a review of methods and data. *Atmos. Environ.* 37, 2173–2191.
- da Silva, M., Monte, M.J.S., Ribeiro, J.R., 1999. Vapour pressures and the enthalpies and entropies of sublimation of five dicarboxylic acids. *J. Chem. Thermodyn.* 31, 1093–1107.
- Elm, J., 2017. Elucidating the limiting steps in sulfuric acid base new particle formation. *J. Phys. Chem. A* 121, 8288–8295.
- Elm, J., Bilde, M., Mikkelsen, K.V., 2012. Assessment of density functional theory in predicting structures and free energies of reaction of atmospheric prenucleation clusters. *J. Chem. Theor. Comput.* 8, 2071–2077.
- Elm, J., Bilde, M., Mikkelsen, K.V., 2013. Assessment of binding energies of atmospherically relevant clusters. *Phys. Chem. Chem. Phys.* 15, 16442–16445.
- Elm, J., Mylllys, N., Olenius, T., Halonen, R., Kurten, T., Vehkamaki, H., 2017. Formation of atmospheric molecular clusters consisting of sulfuric acid and  $\text{C}_8\text{H}_{12}\text{O}_6$  tricarboxylic acid. *Phys. Chem. Chem. Phys.* 19, 4877–4886.
- Frisch, M., Trucks, G., Schlegel, H., Scuseria, G., Robb, M., Cheeseman, J., Scalmani, G., Barone, V., Mennucci, B., Petersson, G., 2013. Gaussian 09, Revision D. 01, 2013. Gaussian Inc., Wallingford CT.
- Ge, X., Wexler, A.S., Clegg, S.L., 2011a. Atmospheric amines - Part I. A review. *Atmos. Environ.* 45, 524–546.
- Ge, X., Wexler, A.S., Clegg, S.L., 2011b. Atmospheric amines - Part II. Thermodynamic properties and gas/particle partitioning. *Atmos. Environ.* 45, 561–577.
- Glasoe, W.A., Volz, K., Panta, B., Freshour, N., Bachman, R., Hanson, D.R., McMurry, P. H., Jen, C., 2015. Sulfuric acid nucleation: an experimental study of the effect of seven bases. *J. Geophys. Res. Atmos.* 120, 1933–1950.
- Hanson, D.R., Eisele, F., 2000. Diffusion of  $\text{H}_2\text{SO}_4$  in humidified nitrogen: hydrated  $\text{H}_2\text{SO}_4$ . *J. Phys. Chem. A* 104, 1715–1719.
- Hanson, D.R., Eisele, F.L., 2002. Measurement of prenucleation molecular clusters in the  $\text{NH}_3$ ,  $\text{H}_2\text{SO}_4$ ,  $\text{H}_2\text{O}$  system. *J. Geophys. Res.-Atmos.* 107, 4158.
- Hanson, D.R., Lovejoy, E.R., 2006. Measurement of the thermodynamics of the hydrated dimer and trimer of sulfuric acid. *J. Phys. Chem. A* 110, 9525–9528.
- He, C., Cheng, J., Zhang, X., Douthwaite, M., Pattison, S., Hao, Z., 2019. Recent advances in the catalytic oxidation of volatile organic compounds: a review based on pollutant sorts and sources. *Chem. Rev.* 119, 4471–4568.
- Hohenberg, P., Kohn, W., 1964. Inhomogeneous electron gas. *Phys. Rev. B* 136, B864.
- Huang, W., Pal, R., Wang, L.-M., Zeng, X.C., Wang, L.-S., 2010a. Isomer identification and resolution in small gold clusters. *J. Chem. Phys.* 132, 054305.
- Huang, W., Sergeeva, A.P., Zhai, H.-J., Averkiev, B.B., Wang, L.-S., Boldyreva, A.I., 2010b. A concentric planar doubly pi-aromatic  $\text{Bi}_9$  cluster. *Nat. Chem.* 2, 202–206.
- Huang, W., Zhai, H.-J., Wang, L.-S., 2010c. Probing the interactions of  $\text{O}_2$  with small gold cluster Anions ( $\text{Au}_n^-$ ,  $n=1$ –7): Chemisorption vs Physisorption. *J. Am. Chem. Soc.* 132, 4344–4351.
- Humphrey, W., Dalke, A., Schulter, K., 1996. Vmd: visual molecular dynamics. *J. Mol. Graph. Model.* 14, 33–38.
- Hunt, S.W., Higgins, K.J., Craddock, M.B., Brauer, C.S., Leopold, K.R., 2003. Influence of a polar near-neighbor on incipient proton transfer in a strongly hydrogen bonded complex. *J. Am. Chem. Soc.* 125, 13850–13860.
- Jimenez, J.L., et al., 2009. Evolution of organic aerosols in the atmosphere. *Science* 326, 1525–1529.
- Johnson, E.R., Keinan, S., Mori-Sanchez, P., Contreras-Garcia, J., Cohen, A.J., Yang, W., 2010. Revealing noncovalent interactions. *J. Am. Chem. Soc.* 132, 6498–6506.
- Karl, M., Leck, C., Gross, A., Pirjola, L., 2012. A study of new particle formation in the marine boundary layer over the central arctic ocean using a flexible multicomponent aerosol dynamic model. *Tellus B* 64, 17158.
- Kawamura, K., Ikushima, K., 1993. Seasonal changes in the distribution of dicarboxylic acids in the urban atmosphere. *Environ. Sci. Technol.* 27, 2227–2235.
- Kerminen, V.M., et al., 2010. Atmospheric nucleation: highlights of the eucaari Project and future directions. *Atmos. Chem. Phys.* 10, 10829–10848.
- Kirkby, J., et al., 2011. Role of sulphuric acid, ammonia and galactic cosmic rays in atmospheric aerosol nucleation. *Nature* 476, 429–433.
- Kittelson, D.B., Watts, W.F., Johnson, J.P., 2004. Nanoparticle emissions on Minnesota highways. *Atmos. Environ.* 38, 9–19.
- Kuang, C., Riipinen, I., Sihot, S.L., Kulmala, M., McCormick, A.V., McMurry, P.H., 2010. An improved criterion for new particle formation in diverse atmospheric environments. *Atmos. Chem. Phys.* 10, 8469–8480.
- Kuerten, A., et al., 2014. Neutral molecular cluster formation of sulfuric acid-dimethylamine observed in real time under atmospheric conditions. *P. Natl. Acad. Sci. USA* 111, 15019–15024.
- Kuerten, A., et al., 2016. Experimental particle formation rates spanning tropospheric sulfuric acid and ammonia abundances, ion production rates, and temperatures. *J. Geophys. Res.-Atmos.* 121, 12377–12400.
- Kulmala, M., 2003. How particles nucleate and grow. *Science* 302, 1000–1001.
- Kulmala, M., Kerminen, V.-M., 2008. On the formation and growth of atmospheric nanoparticles. *Atmos. Res.* 90, 132–150.
- Kulmala, M., Pirjola, U., Makela, J.M., 2000. Stable sulphate clusters as a source of new atmospheric particles. *Nature* 404, 66–69.
- Kulmala, M., Vehkamaki, H., Petaja, T., Dal Maso, M., Lauri, A., Kerminen, V.M., Birmili, W., McMurry, P.H., 2004. formation and growth rates of ultrafine atmospheric particles: a review of observations. *J. Aerosol Sci.* 35, 143–176.
- Kulmala, M., et al., 2012. Measurement of the nucleation of atmospheric aerosol particles. *Nat. Protoc.* 7, 1651–1667.
- Kulmala, M., et al., 2013. Direct observations of atmospheric aerosol nucleation. *Science* 339, 943–946.
- Kurnig, I.J., Scheiner, S., 1987. Ab Initio investigation of the structure of hydrogen halide-amine complexes in the gas phase and in a polarizable medium. *Int. J. Quant. Chem.* 32, 47–56.
- Kurten, T., Loukonen, V., Vehkamaki, H., Kulmala, M., 2008. Amines are likely to enhance neutral and ion-induced sulfuric acid-water nucleation in the atmosphere more effectively than ammonia. *Atmos. Chem. Phys.* 8, 4095–4103.
- Li, H., Kupiainen-Maatta, O., Zhang, H., Zhang, X., Ge, M., 2017. A molecular-scale study on the role of lactic acid in new particle formation: influence of relative humidity and temperature. *Atmos. Environ.* 166, 479–487.
- Lin, X.-X., Liu, Y.-R., Huang, T., Xu, K.-M., Zhang, Y., Jiang, S., Gai, Y.-B., Zhang, W.-J., Huang, W., 2014. Theoretical studies of the hydration reactions of stabilized crieger intermediates from the ozonolysis of beta-pinene. *RSC Adv.* 4, 28490–28498.
- Ling, Y., et al., 2019. Long-term aerosol size distributions and the potential role of volatile organic compounds (VOCs) in new particle formation events in shanghai. *Atmos. Environ.* 202, 345–356.
- Liu, P.S.K., Leaitch, W.R., Banic, C.M., Li, S.M., Ngo, D., Megaw, W.J., 1996. Aerosol observations at chebogue point during the 1993 north atlantic regional experiment: relationships among cloud condensation nuclei, size distribution, and chemistry. *J. Geophys. Res. Atmos.* 101, 28971–28990.
- Liu, Y.-R., Wen, H., Huang, T., Lin, X.-X., Gai, Y.-B., Hu, C.-J., Zhang, W.-J., Huang, W., 2014. Structural exploration of water, nitrate/water, and oxalate/water clusters with basin-hopping method using a compressed sampling technique. *J. Phys. Chem. A* 118, 508–516.
- Liu, L., Li, H., Zhang, H., Zhong, J., Bai, Y., Ge, M., Li, Z., Chen, Y., Zhang, X., 2018. The role of nitric acid in atmospheric new particle formation. *Phys. Chem. Chem. Phys.* 20, 17406–17414.
- Loukonen, V., Kurten, T., Ortega, I.K., Vehkamaki, H., Padua, A.A.H., Sellegrí, K., Kulmala, M., 2010. Enhancing effect of dimethylamine in sulfuric acid nucleation in the presence of water - a computational study. *Atmos. Chem. Phys.* 10, 4961–4974.
- Lu, T., Chen, F., 2012. Multiwfns: a multifunctional wavefunction analyzer. *J. Comput. Chem.* 33, 580–592.
- Lv, S.-S., Miao, S.-K., Ma, Y., Zhang, M.-M., Wen, Y., Wang, C.-Y., Zhu, Y.-P., Huang, W., 2015. Properties and atmospheric implication of methylamine sulfuric acid-water clusters. *J. Phys. Chem. A* 119, 8657–8666.

- Ma, F., Xie, H.-B., Elm, J., Shen, J., Chen, J., Vehkamaki, H., 2019. Piperazine enhancing sulfuric acid-based new particle formation: implications for the atmospheric fate of piperazine. *Environ. Sci. Technol.* 53, 8785–8795.
- Makar, P.A., 2001. The estimation of organic gas vapour pressure. *Atmos. Environ.* 35, 961–974.
- Martinelango, P.K., Dasgupta, P.K., Al-Horr, R.S., 2007. Atmospheric production of oxalic acid/oxalate and nitric acid/nitrate in the tampa bay airshed: parallel pathways. *Atmos. Environ.* 41, 4258–4269.
- McGrath, M.J., Olenius, T., Ortega, I.K., Loukonen, V., Paasonen, P., Kurten, T., Kulmala, M., Vehkamaki, H., 2012. Atmospheric cluster dynamics Code: a flexible method for solution of the birth-death equations. *Atmos. Chem. Phys.* 12, 2345–2355.
- McGregor, K.G., Anastasio, C., 2001. Chemistry of fog waters in California's central valley: 2. Photochemical transformations of amino acids and alkyl amines. *Atmos. Environ.* 35, 1091–1104.
- Metzger, A., et al., 2010. Evidence for the role of organics in aerosol particle formation under atmospheric conditions. *P. Natl. Acad. Sci. USA* 107, 6646–6651.
- Miao, S.-K., Jiang, S., Chen, J., Ma, Y., Zhu, Y.-P., Wen, Y., Zhang, M.-M., Huang, W., 2015. Hydration of a sulfuric acid-oxalic acid complex: acid dissociation and its atmospheric implication. *RSC Adv.* 5, 48638–48646.
- Myllys, N., Chee, S., Olenius, T., Lawler, M., Smith, J., 2019. Molecular-level understanding of synergistic effects in sulfuric acid-amine-ammonia mixed clusters. *J. Phys. Chem. A* 123, 2420–2425.
- Nadykto, A.B., Yu, F., 2007. Strong hydrogen bonding between atmospheric nucleation precursors and common organics. *Chem. Phys. Lett.* 435, 14–18.
- Nadykto, A.B., Yu, F., Jakovleva, M.V., Herb, J., Xu, Y., 2011. Amines in the earth's atmosphere: a density functional theory study of the thermochemistry of pre-nucleation clusters. *Entropy* 13, 554–569.
- Nadykto, A.B., Herb, J., Yu, F., Xu, Y., Nazarenko, E.S., 2015. Estimating the lower limit of the impact of amines on nucleation in the earth's atmosphere. *Entropy* 17, 2764–2780.
- Olenius, T., et al., 2013. Comparing simulated and experimental molecular cluster distributions. *Faraday Discuss.* 165, 75–89.
- Paasonen, P., et al., 2010. On the roles of sulphuric acid and low-volatility organic vapours in the initial steps of atmospheric new particle formation. *Atmos. Chem. Phys.* 10, 11223–11242.
- Peng, X.-Q., Liu, Y.-R., Huang, T., Jiang, S., Huang, W., 2015. Interaction of gas phase oxalic acid with ammonia and its atmospheric implications. *Phys. Chem. Chem. Phys.* 17, 9552–9563.
- Prenti, A.J., DeMott, P.J., Kreidenweis, S.M., Sherman, D.E., Russell, L.M., Ming, Y., 2001. The effects of low molecular weight dicarboxylic acids on cloud formation. *J. Phys. Chem. A* 105, 11240–11248.
- Saxena, P., Hildemann, L.M., 1996. Water-soluble organics in atmospheric particles: a critical review of the literature and application of thermodynamics to identify candidate compounds. *J. Atmos. Chem.* 24, 57–109.
- Saxon, A., Diaz-Sanchez, D., 2005. Air pollution and allergy: you are what you breathe. *Nat. Immunol.* 6, 223–226.
- Schade, G.W., Crutzen, P.J., 1995. Emission of aliphatic-amines from animal husbandry and their reactions - potential source of  $\text{N}_2\text{O}$  and HCN. *J. Atmos. Chem.* 22, 319–346.
- Schoobesberger, S., et al., 2013. Molecular understanding of atmospheric particle formation from sulfuric acid and large oxidized organic molecules. *P. Natl. Acad. Sci. USA* 110, 17223–17228.
- Schoobesberger, S., et al., 2015. On the composition of ammonia-sulfuric-acid ion clusters during aerosol particle formation. *Atmos. Chem. Phys.* 15, 55–78.
- Smith, J.N., Dunn, M.J., VanReken, T.M., Iida, K., Stolzenburg, M.R., McMurry, P.H., Huey, L.G., 2008. Chemical composition of atmospheric nanoparticles formed from nucleation in tecamac, Mexico: evidence for an important role for organic species in nanoparticle growth. *Geophys. Res. Lett.* 35, L04808.
- Smith, J.N., Barsanti, K.C., Friedli, H.R., Ehn, M., Kulmala, M., Collins, D.R., Scheckman, J.H., Williams, B.J., McMurry, P.H., 2010. Observations of aminium salts in atmospheric nanoparticles and possible climatic implications. *P. Natl. Acad. Sci. USA* 107, 6634–6639.
- Wales, D.J., Doye, J.P.K., 1997. Global optimization by basin-hopping and the lowest energy structures of Lennard-Jones clusters containing up to 110 atoms. *J. Phys. Chem. A* 101, 5111–5116.
- Wang, L., Khalizov, A.F., Zheng, J., Xu, W., Ma, Y., Lal, V., Zhang, R., 2010. Atmospheric nanoparticles formed from heterogeneous reactions of organics. *Nat. Geosci.* 3, 238–242.
- Wen, H., Liu, Y.-R., Xu, K.-M., Huang, T., Hu, C.-J., Zhang, W.-J., Huang, W., 2014. Probing the 2D-to-3D structural transition in gold clusters with a single sulfur atom:  $\text{Au}_x\text{S}^{0,\pm 1}$  ( $x=1\text{--}10$ ). *RSC Adv.* 4, 15066–15076.
- Xie, H.-B., Elm, J., Halonen, R., Mylllys, N., Kurten, T., Kulmala, M., Vehkamaki, H., 2017. Atmospheric fate of monoethanolamine: enhancing new particle formation of sulfuric acid as an important removal process. *Environ. Sci. Technol.* 51, 8422–8431.
- Xu, Y., Nadykto, A.B., Yu, F., Jiang, L., Wang, W., 2010a. formation and properties of hydrogen-bonded complexes of common organic oxalic acid with atmospheric nucleation precursors. *J. Mol. Struc-theochem* 951, 28–33.
- Xu, Y., Nadykto, A.B., Yu, F., Herb, J., Wang, W., 2010b. Interaction between common organic acids and trace nucleation species in the earth's atmosphere. *J. Phys. Chem. A* 114, 387–396.
- Xu, K.-M., Huang, T., Wen, H., Liu, Y.-R., Gai, Y.-B., Zhang, W.-J., Huang, W., 2013. A density functional study of phosphorus-doped gold clusters:  $\text{Au}_n\text{P}$  ( $n=1\text{--}8$ ). *RSC Adv.* 3, 24492–24502.
- Xu, J., Finlayson-Pitts, B.J., Gerber, R.B., 2017. Proton transfer in mixed clusters of methanesulfonic acid, methylamine, and oxalic acid: implications for atmospheric particle formation. *J. Phys. Chem. A* 121, 2377–2385.
- Yoon, J.-W., Park, J.-H., Shur, C.-C., Jung, S.-B., 2007. Characteristic evaluation of electroless nickel-phosphorus deposits with different phosphorus contents. *Microelectron. Eng.* 84, 2552–2557.
- Yu, F.Q., 2006. Effect of ammonia on new particle formation: a kinetic  $\text{H}_2\text{SO}_4\text{-H}_2\text{O-NH}_3$  nucleation model constrained by laboratory measurements. *J. Geophys. Res. Atmos.* 111 (D1), D01204.
- Yu, F.Q., Turco, R.P., 2000. Ultrafine aerosol formation via ion-mediated nucleation. *Geophys. Res. Lett.* 27, 883–886.
- Yu, H., McGraw, R., Lee, S.-H., 2012. Effects of amines on formation of sub-3 nm particles and their subsequent growth. *Geophys. Res. Lett.* 39, L02807.
- Yu, F., Nadykto, A.B., Herb, J., Luo, G., Nazarenko, K.M., Uvarova, L.A., 2018.  $\text{H}_2\text{SO}_4\text{-H}_2\text{O-NH}_3$  ternary ion-mediated nucleation (TIMN): kinetic-based model and comparison with cloud measurements. *Atmos. Chem. Phys.* 18, 17451–17474.
- Yue, D.L., Hu, M., Zhang, R.Y., Wang, Z.B., Zheng, J., Wu, Z.J., Wiedensohler, A., He, L., Y., Huang, X.F., Zhu, T., 2010. The roles of sulfuric acid in new particle formation and growth in the mega-city of beijing. *Atmos. Chem. Phys.* 10, 4953–4960.
- Zhang, R., 2010. Getting to the critical nucleus of aerosol formation. *Science* 328, 1366–1367.
- Zhang, R.Y., Suh, I., Zhao, J., Zhang, D., Fortner, E.C., Tie, X.X., Molina, L.T., Molina, M. J., 2004. Atmospheric new particle formation enhanced by organic acids. *Science* 304, 1487–1490.
- Zhang, R., Khalizov, A., Wang, L., Hu, M., Xu, W., 2012. Nucleation and growth of nanoparticles in the atmosphere. *Chem. Rev.* 112, 1957–2011.
- Zhang, H., Kupiainen-Maatta, O., Zhang, X., Molinero, V., Zhang, Y., Li, Z., 2017. The enhancement mechanism of glycolic acid on the formation of atmospheric sulfuric acid-ammonia molecular clusters. *J. Chem. Phys.* 146 (18), 184308.
- Zhang, W., Ji, Y., Li, G., Shi, Q., An, T., 2019. The heterogeneous reaction of dimethylamine/ammonia with sulfuric acid to promote the growth of atmospheric nanoparticles. *Environ. Sci.-Nano* 6, 2767–2776.
- Zhao, Y., Truhlar, D.G., 2008. The M06 suite of density functionals for main group thermochemistry, thermochemical kinetics, noncovalent interactions, excited states, and transition elements: two new functionals and systematic testing of four M06-class functionals and 12 other functionals. *Theor. Chem. Acc.* 120, 215–241.
- Zhao, J., Smith, J.N., Eisele, F.L., Chen, M., Kuang, C., McMurry, P.H., 2011. Observation of neutral sulfuric acid-amine containing clusters in laboratory and ambient measurements. *Atmos. Chem. Phys.* 11, 10823–10836.